



THE UNIVERSITY *of* EDINBURGH

Edinburgh Research Explorer

Boreal forest floor greenhouse gas emissions across a Pleurozium schreberi-dominated, wildfire-disturbed chronosequence

Citation for published version:

Mason, K, Oakley, S, Street, L, Arróniz-Crespo, M, Jones, D, DeLuca, T & Ostle, N 2019, 'Boreal forest floor greenhouse gas emissions across a Pleurozium schreberi-dominated, wildfire-disturbed chronosequence', *Ecosystems*. <https://doi.org/10.1007/s10021-019-00344-2>

Digital Object Identifier (DOI):

[10.1007/s10021-019-00344-2](https://doi.org/10.1007/s10021-019-00344-2)

Link:

[Link to publication record in Edinburgh Research Explorer](#)

Document Version:

Peer reviewed version

Published In:

Ecosystems

General rights

Copyright for the publications made accessible via the Edinburgh Research Explorer is retained by the author(s) and / or other copyright owners and it is a condition of accessing these publications that users recognise and abide by the legal requirements associated with these rights.

Take down policy

The University of Edinburgh has made every reasonable effort to ensure that Edinburgh Research Explorer content complies with UK legislation. If you believe that the public display of this file breaches copyright please contact openaccess@ed.ac.uk providing details, and we will remove access to the work immediately and investigate your claim.



**Boreal forest floor greenhouse gas emissions across a
Pleurozium schreberi-dominated, wildfire-disturbed
chronosequence**

Journal:	<i>Ecosystems</i>
Manuscript ID	ECO-18-0205.R2
Types:	Original Article
Date Submitted by the Author:	28-Nov-2018
Complete List of Authors:	Mason, Kelly; Centre for Ecology & Hydrology, Oakley, Simon; Centre for Ecology and Hydrology, Soil Ecology Street, Lorna; University of Edinburgh School of GeoSciences Arroniz-Crespo, Maria; Universidad Politecnica de Madrid, Química y Tecnología de Alimentos Jones, David; Bangor University College of Natural Sciences, School of Environment, Natural Resources and Geography DeLuca, Thomas; University of Montana, WA Franke College of Forestry and Conservation Ostle, Nick; Lancaster University, Lancaster Environment Centre
Key Words:	boreal forest, wildfire disturbance, greenhouse gas emissions, carbon dynamics, chronosequence, forest floor

Boreal forest floor greenhouse gas emissions across a *Pleurozium schreberi*-dominated, wildfire-disturbed chronosequence

Shortened title for page headings: Boreal forest floor GHG fluxes in later succession

Kelly E. Mason,^{1*} Simon Oakley,¹ Lorna E. Street,² María Arróniz-Crespo,^{3,4} David L. Jones,⁴ Thomas H. DeLuca,⁵ and Nicholas J. Ostle⁶

¹Centre for Ecology & Hydrology, Lancaster Environment Centre, Library Avenue, Bailrigg, Lancaster LA1 4AP, UK

²School of GeoSciences, University of Edinburgh, Edinburgh, UK

³Departamento de Química y Tecnología de Alimentos, Universidad Politécnica de Madrid, Madrid, Spain

⁴School of Environment, Natural Resources and Geography, Bangor University, Bangor, UK

⁵WA Frank College of Forestry and Conservation, University of Montana, Missoula, USA

⁶Lancaster Environment Centre, Lancaster University, Lancaster LA1 4YQ, UK

Abstract

The boreal forest is a globally critical biome for carbon cycling. Its forests are shaped by wildfire events that affect ecosystem properties and climate feedbacks including greenhouse gas (GHG) emissions. Improved understanding of boreal forest floor processes is needed to predict the impacts of anticipated increases in fire frequency, severity, and extent. In this study, we examined relationships between time since last wildfire (TSF), forest floor soil properties, and greenhouse gas emissions (CO₂, CH₄, N₂O) along a *Pleurozium schreberi*-dominated chronosequence in mid- to late succession located in northern Sweden. Over three growing seasons in 2012-2014, GHG flux measurements were made *in situ* and samples were collected for laboratory analyses. We predicted that *P. schreberi*-covered forest floor GHG fluxes would be related to distinct trends in the soil properties and microbial community along the wildfire chronosequence. Although we found no overall effect of TSF on GHG emissions, there was evidence that soil C:N, one of the few properties to show a trend with time, was inversely linked to ecosystem respiration. We also found that local microclimatic conditions and site-dependent properties were better predictors of GHG fluxes than TSF. This shows that site-dependent co-variables (i.e. forest floor climate and plant-soil properties) need to be considered as well as TSF to predict GHG emissions as wildfires become more frequent, extensive and severe.

Key words: boreal forest; wildfire disturbance; greenhouse gas emissions; carbon dynamics; forest floor; chronosequence

Introduction

Occupying 11% of the global land surface, boreal forests represent Earth's largest terrestrial biome and provide habitats for uniquely adapted biodiversity (Wardle and others 2003). These forests are estimated to hold 32% of global forest ecosystem carbon (C) stocks (Pan and others 2011) and play a major role in global greenhouse gas (GHG) dynamics (McNamara and others 2015). Wildfire is a major driver of change in the boreal region, turning the forest from a sink to a source of C through its release to the atmosphere, mainly in the form of CO₂ but also as methane (CH₄), carbon monoxide, and particulate C (Flannigan and others 2005). However, there is currently little information on how wildfire history influences forest floor GHG emissions.

Boreal forests are also particularly vulnerable to climate change with warming and reduced precipitation predicted to lengthen the fire season, increase fuel load, and reduce fuel moisture (Kovats and others 2014). These conditions have the potential to increase the frequency, intensity, severity, and extent of wildfires in the boreal region (de Groot and others 2013; Flannigan and others 2013), although fire suppression by human activity and land-use change may counteract this to some degree (Niklasson and Granstrom 2000; Girardin and others 2009). Understanding the mechanisms underpinning the recovery of these ecosystems is important for predicting how an overall increase in fire activity will contribute to global GHG emissions.

Boreal forests are characteristically nutrient poor, but fire releases nutrients, such as nitrogen (N), locked up in living biomass back into the system (Harden and others 2002; DeLuca and others 2002a; 2008). In the years following burning, this nutrient flush is essential for the growth of new biomass and recovery of C stocks. This fertile early successional stage, with plant communities of high litter quality and rapid turnover supporting belowground microbial biomass and decomposition processes (Wardle and Zackrisson 2005), transitions into a slower stage of recovery after several decades (Chapin and others 2002, Ward and others 2014).

1
2
3 In later succession, decreasing nutrient availability slows the growth of biomass and leads to changes
4 in the forest floor plant communities, upon which belowground activity is highly dependent (Wardle
5 1997). In these stands, forest floor vegetation is dominated by slow-growing species with more
6 recalcitrant litter. In particular, the feather mosses *Pleurozium schreberi* (Bird.) Mitt and
7
8
9
10
11 *Hylocomium splendens* can take several decades to establish but then often cover up to 70-100% of
12 the ground surface (Engelmark 1999; DeLuca and others 2002a; Zackrisson and others 2004; Street
13 and others 2013). These mosses contain N-fixing cyanobacteria that contribute to the accumulation
14 and cycling of an otherwise limiting nutrient in the system (DeLuca and others 2002b; Zackrisson and
15 others 2009) and influence belowground microbial processes by altering conditions such as soil
16 moisture and temperature (Oechel and Van Cleve 1986; Bonan and Shugart 1989; Williams and
17 Flanagan 1996).

18
19
20
21
22
23
24
25
26
27
28 Despite substantial work done to understand forest floor ecosystem properties in a post-fire
29 chronosequence of forested Swedish boreal islands that have not experienced fire for hundreds up to
30 thousands of years (for example, Wardle 1997; Wardle and others 2003, 2012a, 2012b; Lagerström
31 and others 2009; Clemmensen and others 2013, 2015; McNamara and others 2015), only a few studies
32 have looked at trends in post-fire forest floor recovery in the wider boreal landscape of northern
33 Europe (Zackrisson and others 1996; DeLuca and others 2002a, Zackrisson and others 2004), where
34 the fire return interval is approximately 200-300 years (Carcaillet and others 2007). Although some
35 evidence suggests that rapid early changes in forest floor ecosystem properties reach a “steady state”
36 several decades after fire (Ward and others 2014), other evidence shows that more gradual changes
37 continue over longer periods of time (Paré and others 1993; DeLuca and others 2002a; O’Neill and
38 others 2003; Zackrisson and others 2004). To date, no studies have examined the relationship
39 between *in situ* GHG fluxes and boreal forest floor properties across a wildfire chronosequence in
40 mid- to late succession in northern Europe.

41
42
43
44
45
46
47
48
49
50
51
52 In this study, we wanted to determine the relationships between time since last wildfire (hereafter
53 ‘time since fire’, TSF), soil properties, and forest floor GHG emissions of CO₂, CH₄, and N₂O in
54
55
56
57
58
59
60

1
2
3 *Pleurozium schreberi*-dominated boreal forest stands in mid-late succession. We achieved this using
4 a wildfire-disturbed chronosequence located in northern Sweden consisting of six sites ranging from
5 47 to 367 years since last wildfire. These sites form part of a larger chronosequence used in previous
6 works, which have shown increased feathermoss cover and associated N-fixation with increasing
7 TSF, as well as reduced nitrification, ammonification, and N mineralization (DeLuca and others
8 2002a, Zackrisson and others 2004). We collected forest floor samples and measurements during the
9 growing season over three years between 2012 and 2014. Our objectives were to explore whether *P.*
10 *schreberi* had an effect on forest floor GHG emissions with increasing TSF and to examine whether
11 changes in forest floor soil properties and local climatic factors account for variance in these GHG
12 emissions. We hypothesized TSF would be an important predictor of *P. schreberi*-dominated forest
13 floor GHG fluxes as a result of associated changes in soil properties. Specifically, we expected that
14 with increasing TSF, CO₂ fluxes would increase with the buildup of the organic soil horizon, CH₄
15 influx would increase as in McNamara and others (2015), and that N₂O fluxes would increase in
16 relation to increased *P. schreberi* cover and associated increases in N₂-fixation.
17
18
19
20
21
22
23
24
25
26
27
28
29
30
31
32
33
34

35 **Methods**

36 *Field sites and microclimate measurements*

37
38
39 The field sites for this project were located in the Northern Boreal zone of Sweden. They comprised a
40 subset of six forest reserve stands of varying age since last wildfire (i.e. 47-367 years) selected from a
41 chronosequence of sites that had previously been dated using tree ring scars (Zackrisson 1980) (Table
42 1; site ages are TSF as of 2014). The sites were selected at locations with a similar soil type
43 (developed in granitic glacial till or sediment, with a 2-10 cm thick Oa/Oe horizon, 10-20 thick cm E
44 horizon, and 30-40 cm thick Bs horizon, classified as either Typic or Entic Haplocryods; DeLuca and
45 others 2002a) and vegetation composition (i.e. Scots pine (*Pinus sylvestris*), Norway spruce (*Picea*
46 *abies*)), and a ground vegetation of dwarf shrubs (i.e. *Vaccinium* sp., *Empetrum* sp., and *Calluna* sp.)
47 and feather mosses (i.e. *P. schreberi* and *H. splendens*). Weather stations measuring air temperature,
48 soil temperature at 1 cm and 5 cm depth, soil moisture, and surface leaf moisture (Decagon Devices,
49
50
51
52
53
54
55
56
57
58
59
60

1
2
3 Inc, USA) were installed at all sites. Microclimate data was collected between June 2012 and July
4
5 2014.
6
7
8

9
10 *Forest floor greenhouse gas fluxes*

11 To measure forest floor greenhouse gas fluxes (i.e. excluding trees), five permanent PVC collars (30
12 cm diameter, 10 cm height) were installed along a 50-100 m transect at each site. Collar locations
13 were selected at 10-20 m distance intervals, on a mat of *P. schreberi*. These were left for two days
14 before the first sets of GHG flux measurements were made. Plots were sampled once in June 2012
15 and twice in each following sampling campaign (September 2012, June 2013, and July 2014). Gas
16 fluxes were measured following the methods of Ward and others (2013). Briefly, forest floor
17 ecosystem respiration (ER) and net ecosystem exchange (NEE) were measured over 2 minute
18 intervals using a portable infrared gas analyser (PP Systems EGM4) connected to an opaque or clear
19 chamber lid (35 cm height), respectively. For NEE, measurements were made of photosynthetically
20 active radiation (PAR) at the height of forest floor vegetation using a PAR Quantum Sensor (Skye
21 Instruments, UK). NEE is the combination of ER and gross primary productivity (GPP), such that a
22 negative value for NEE indicates that GPP is greater than ER (i.e. CO₂ is being sequestered) while a
23 positive value indicates that ER is greater (i.e. net CO₂ is being released). Forest floor CH₄ and N₂O
24 fluxes were measured using a closed static chamber approach, whereby opaque chamber lids were
25 sealed and headspace samples (10 mL) were taken using a gas syringe every ten minutes over half an
26 hour and immediately injected into evacuated 3 mL Exetainer® vials (Labco Ltd, UK). Samples were
27 analysed in the laboratory on a PerkinElmer Autosystem XL gas chromatograph (GC) with an FID for
28 CH₄, an electron capture detector for N₂O and argon carrier gas. Sample peak areas were converted to
29 part per million (ppm) concentrations using a standard curve based on three calibrated gas standard
30 mixtures (BOC, UK). Results were corrected for instrumental drift as required. Gas concentration
31 data from the GC were transformed from parts per million to flux of mg CH₄-C or mg N₂O-N m⁻² hr⁻¹.
32
33 Quality control procedures were implemented to identify missing data values or effects of
34 atmospheric contamination of stored samples (all methods from Ward and others 2013).
35
36
37
38
39
40
41
42
43
44
45
46
47
48
49
50
51
52
53
54
55
56
57
58
59
60

Plant and soil sampling and analyses

Following the final round of GHG flux sampling in 2014, gas sampling plots were destructively harvested. All aboveground plant material within the gas chamber collars was collected, dried at 60°C, and weighed for total dry weight biomass. One soil core (5 cm diameter, 10 cm depth) was taken from the centre of the collar to measure soil horizon depth, bulk density, and total soil C and N content. Estimates of cover by individual plant species were made where plants were often overlaid, creating >100% cover. In June 2012, six soil cores were collected along a transect for measurements of inorganic nitrogen (i.e. NO_3^- , NH_4^+). In September 2013, four additional cores were collected for analysis of more soil properties, including pH, total phosphorous (P), loss on ignition (as a measure of organic matter content), and microbial PLFA content (as described below) of the soil organic horizon at each site.

To determine microbial biomass and fungal/bacterial ratios, soil samples were extracted following a modified Bligh and Dyer (1959) method, as described by Crossman and others (2004). Briefly, lipids were extracted from freeze-dried, finely ground soil samples using Bligh and Dyer extractants and a citrate buffer, then separated into neutral, free fatty acids, and phospholipids on a silica solid phase extraction column. Mild alkaline methylation of the phospholipids produced fatty acid methyl esters for analysis. Once suspended in hexane, 1 μL PLFA samples were analysed on an Agilent Technologies (UK) 6890 GC equipped with a CP-Sil 5CB fused-silica capillary column (50 m x 0.32 mm i.d. x 0.25 μm) and flame ionization detector (FID). Sample PLFA peaks were identified based on known relative retention times, calculated as a proportion of the internal standard C19:0 methyl nonadecanoate, and converted to $\text{nmol PLFA g}_{\text{dw}}^{-1}$. Bacterial PLFAs were identified by terminal and mid-chain branched fatty acids (15:0i, 15:0a, 16:0i, 17:0i, 17:0a) or cyclopropyl saturated and monosaturated fatty acids (16:1 ω 7, 7,cy-17:0, 18:1 ω 7, 7,8cy-19:0), while fungal PLFAs were identified as 18:2 ω 6,9. The concentration of total PLFAs was calculated using all identified peaks (Whitaker and others 2014).

Statistical analysis

Statistical analyses were executed to determine the significance of a) relationships between TSF and site forest floor properties, and b) key ecosystem properties as predictors of forest floor GHG emissions. All statistical analyses were performed in R software (R Development Core Team 2014).

Soil and plant properties along the chronosequence

Linear regression analyses were carried out to determine trends in some forest floor properties with increasing TSF. These were carried out on soil collected both from within the gas sampling collars and along the transects, as well as on *P. schreberi* cover and total aboveground biomass from within the sampling rings. If required, data were transformed to meet model assumptions. To correct for multiple comparisons, a false discovery rate (FDR) correction was applied to *p*-values using the Benjamini-Hochberg critical value for FDR of 0.25.

Linear mixed effects modelling to predict GHG fluxes

Linear mixed effects (LME) models were developed to examine controls on forest floor GHG fluxes. Before looking at more complex models, we created simple LME models for individual sampling campaigns to determine trends in GHG fluxes with increasing TSF (nlme package, Pinheiro and others 2015). For this, GHG flux response was modelled with TSF as a fixed effect and plot as a random effect for repeated sampling. Again, data were transformed where necessary to meet model assumptions and the FDR correction was applied to *p*-values. Parameter estimates were obtained through a restricted maximum likelihood (REML) estimation of the models. *P*-values were obtained through likelihood ratio tests of each model compared to the same model minus TSF as a fixed effect, both created using a maximum likelihood (ML) estimation. R^2 values for each model were obtained using the MuMIn package (Bartoń 2016)

Following the simple mixed effects modelling procedure, it was determined that the GHG flux responses measured did not show any consistent trends with increasing TSF; therefore, two sets of

1
2
3 models containing the other measured parameters were subsequently developed: one set containing
4
5 TSF (continuous) as a fixed effect, and the other set using site (discrete).
6
7
8

9
10 The models were developed using the following approach. To begin, a correlation matrix was used to
11
12 identify factors showing collinearity (>70% correlated) and one of each collinear pair was excluded
13
14 from the initial model. To examine the effects of site-specific microclimates on forest floor
15
16 greenhouse gas fluxes, weather station data was incorporated into the LME models. This, however,
17
18 meant data was reduced to five sites as GUO had no weather station. After removing collinear
19
20 weather station variables, we included the following data averaged over one hour prior to sampling:
21
22 mean soil temperature at 5 cm depth, mean soil moisture, and mean surface leaf moisture. Although
23
24 plant species cover was recorded, only final aboveground biomass and percent cover of *P. schreberi*
25
26 were included in the models due to collars being placed selectively on *P. schreberi* mats rather than
27
28 randomly, covering natural variation in plant cover. The final selection of factors included in the
29
30 initial models are summarized in Table 2. Next, random effects were included in the models to
31
32 account for repeated sampling at each plot and unequal variances between sites (Zuur and others
33
34 2009). Using ML estimations, fixed effects selection was performed using single term deletions and
35
36 chi-squared likelihood ratio (LR) tests, where factors with non-significant effects ($p > 0.05$) were
37
38 sequentially removed from the model. Again, likelihood ratio deletion tests (LRTs) determined the
39
40 significance of retained factors by comparing the selected model with that same model but with the
41
42 factor removed. If single terms were included in significant interactions, the interaction was also
43
44 dropped before testing LRs (Zuur and others 2009; De Vries and others 2012). Finally, the models
45
46 were fit using REML estimations to obtain parameter estimates.
47
48
49
50
51
52

53 **Results**

54 Soil properties and plant composition

55
56
57
58
59
60

1
2
3 We measured a range of soil metrics to determine whether differences in soil organic horizon
4 properties underlying mats of *P. schreberi* differed across the chronosequence. Linear regression
5 analyses showed C:N at these six sites to increase with TSF, both within the GHG rings ($R^2 = 0.153$, p
6 < 0.033) and from the other samples taken along the transects ($R^2 = 0.233$, $p < 0.020$). Also from
7 samples taken along the transects, total N ($R^2 = 0.181$, $p < 0.043$) and NH_4^+ ($R^2 = 0.190$, $p < 0.008$)
8 decreased with increasing TSF; however, this was not seen in the samples taken from the GHG rings
9 (Figure 1). No other properties showed significant changes with TSF (Figure S1).
10
11
12
13
14
15
16
17
18
19

20 Measurements of plant aboveground biomass and percent cover of *P. schreberi* were taken from
21 within the gas sampling rings at each site. Total aboveground biomass did not change with TSF,
22 while *P. schreberi* cover ranged from 70-100% in the youngest site and increased to 100% in the two
23 oldest sites (Figure S2).
24
25
26
27
28
29
30

31 Greenhouse gas fluxes

32 The results of simple mixed effects models on the various GHG fluxes with age are presented in
33 Figure 2. Mean rates of ER were in the range of 20 to 120 mg $\text{CO}_2\text{-C m}^{-2} \text{ hr}^{-1}$. July 2014 showed
34 higher overall fluxes and was the only sampling campaign to show a trend for ER (decreasing) with
35 increasing TSF ($-0.144 \cdot \text{year}^{-1} \pm 0.04$ (SE), $R^2_{\text{marginal}} = 0.204$, $df = 4$, $p < 0.001$). Mean NEE fluxes
36 ranged from about -42 to +33 mg $\text{CO}_2\text{-C m}^{-2} \text{ hr}^{-1}$, where negative values equate to a net sink and
37 positive values represent a net source of CO_2 . In June 2013 alone, NEE showed a slight but weak
38 increasing trend with TSF ($0.098 \cdot \text{year}^{-1} \pm 0.048$ (SE), $R^2_{\text{marginal}} = 0.084$, $df = 4$, $p < 0.049$). Mean
39 methane flux rates were all negative, ranging from approximately -73 to -2 $\mu\text{g CH}_4\text{-C m}^{-2} \text{ hr}^{-1}$,
40 suggesting a net oxidation of CH_4 . Regression analyses showed weak trends of small increases in
41 CH_4 flux with stand TSF in June 2013 ($0.063 \cdot \text{year}^{-1} \pm 0.031$ (SE), $R^2_{\text{marginal}} = 0.097$, $p < 0.039$) and
42 July 2014 ($0.108 \cdot \text{year}^{-1} \pm 0.050$ (SE), $R^2_{\text{marginal}} = 0.127$, $p < 0.030$). N_2O fluxes ranged from -3 to +4
43 $\mu\text{g N}_2\text{O-N m}^{-2} \text{ hr}^{-1}$ and did not vary significantly across sites.
44
45
46
47
48
49
50
51
52
53
54
55
56
57
58
59
60

1
2
3 Because there was not a consistent linear effect of TSF on soil properties or GHG fluxes, we have
4 focussed on presenting GHG flux models created using site (discrete) rather than TSF. However,
5 results of the flux models created using TSF are presented in Tables S1-S2. No significant model was
6 found for N₂O fluxes when TSF was used as a fixed effect.
7
8
9
10

11
12
13 The model results (using site) for the different gas fluxes are summarized in Tables 3 and 4. The site
14 x soil temperature interaction was significant for NEE, with soil temperature correlated with increases
15 in NEE (i.e. lower uptake of CO₂). Site was a significant factor for ER, CH₄, and N₂O fluxes. ER,
16 NEE, and CH₄ flux also varied across different sampling campaigns. Related to recent condensation
17 and precipitation, increases in mean leaf surface moisture around the time of sampling were
18 negatively related to ER and CH₄ flux but positively related to N₂O flux; however, increased soil
19 moisture was strongly associated with higher ER and also linked to lower N₂O. Soil properties were
20 significant in only two of the GHG flux models (Table 3); ER was negatively related to C:N while
21 NEE decreased (i.e. higher uptake of CO₂) with increased organic horizon depth.
22
23
24
25
26
27
28
29
30
31
32
33
34
35
36

37 **Discussion**

38
39
40
41 In this study, we set out to determine whether soil properties of *P. schreberi*-dominated boreal forest
42 stands in mid- to late succession show patterns of change that could be used along with TSF and
43 microclimatic data to predict forest floor GHG fluxes. We found that properties of the soil organic
44 horizon, to which post-fire changes to soil C and nutrients are largely restricted (Holden and others
45 2013), varied amongst the six sites. There were some weak trends in soil properties with TSF; C:N
46 showed a small increase with time since fire while NH₄⁺ and total N content decreased. Due to
47 equipment, logistical, and time limitations associated with closed-chamber gas sampling, we were
48 forced to select six chronosequence sites, so it is likely that the number and age range of our sites
49 were not great enough to capture many significant differences. In a prior study using this
50 chronosequence, eight sites (including three from this study) were used and some differences in soil
51
52
53
54
55
56
57
58
59
60

1
2
3 variables were indeed observed with TSF (DeLuca and others 2002a). Of the few observed changes
4
5 in soil properties with increasing TSF, the increasing ratio of C to N was associated with lower ER
6
7 fluxes in our study. This result indicates that higher natural soil N is associated with enhanced soil
8
9 microbial activity, which has been seen with N addition studies in other low-N systems (Jonasson and
10
11 others 1999; Allison and others 2008). However, there was no such relationship observed with total
12
13 N, and some research suggests that total C:N is not a good indicator of humus decomposition, which
14
15 can be more dependent on the quality of C rather than N availability (e.g. bound up in N-polyphenol
16
17 complexes that inhibit production of complex-C degrading enzymes) (Prescott and others 2000;
18
19 Hobbie and others 2002; DeLuca and Boisvenue 2012).

20
21
22
23
24 We found that forest floor GHG fluxes showed minor, intermittent trends across the wildfire
25
26 chronosequence. There was some evidence of decreased ER and increased NEE on two separate
27
28 sampling campaigns. The decrease in the influx of CH₄ with increasing TSF, as observed on two
29
30 sampling campaigns, was small but statistically significant. This is contrary to the results of
31
32 McNamara and others (2015), who found an increase in the CH₄ sink capacity of boreal soils with
33
34 increasing TSF in the aforementioned chronosequence of island sites in northern Sweden. One reason
35
36 for this could be in part due to the higher amount of *P. schreberi* cover in older stands, as some
37
38 mosses are known to emit small amounts of CH₄ (Lenhart and others 2015).

39
40
41
42
43 The site x soil temperature interaction was significant in the LME model of NEE, suggesting that the
44
45 effect of a rise in temperature varied from site to site. One explanation for this could be that the
46
47 temperature sensitivities (Q_{10}) of the forest floor community vary amongst the sites, since the
48
49 respiration activity of soil microbial communities (Briones and others 2014) and plants (Tjoelker and
50
51 others 2008) can acclimate under different conditions. For instance, FET (215 years since fire)
52
53 consistently experienced higher average annual temperatures than other sites (data not shown) and had
54
55 the lowest ER and CH₄ consumption in July 2014 (Figure 2), which was much warmer and drier than
56
57 the other sampling periods. It is possible that the microbial community at FET is less sensitive to
58
59 warmer temperatures than those at other sites and therefore had a smaller response to higher
60

1
2
3 temperatures. In relation to this, sampling period was highly significant in ER, NEE, and CH₄ fluxes,
4 highlighting the importance of overall climatic conditions at the time of sampling. Again, evidence of
5 this was seen in July 2014, which had higher ER and NEE fluxes as well as higher CH₄ consumption
6 corresponding to warm, dry conditions (Figure 2). Notably, compared to other sites, the youngest site
7 (NJA, 47 years since fire) had exceptionally low (i.e. highly negative) NEE linked to high
8 photosynthetic activity during this period. This is likely the result of higher grass biomass (data not
9 shown), which is much faster-growing than the feathermoss or shrub species.

10
11
12
13
14
15
16
17
18
19
20 Ecosystem respiration showed a strong positive response to soil moisture, which is known to be
21 important for microbial activity and plant productivity in boreal systems (Williams and Flanagan
22 1996; DeLuca and Boisvenue 2012; Van Cleve and Sprague 2015). Although soil moisture, a driver
23 of methane oxidation in boreal soils (McNamara and others 2015), did not appear to influence our
24 CH₄ fluxes, increases in leaf moisture were associated with greater CH₄ influx. Leaf and soil moisture
25 were both significantly linked to N₂O fluxes; however, this model had a very low R² value, resulting
26 in low confidence in its use as a predictor of N₂O fluxes and highlighting the complexity of the N
27 cycle in this system.

28
29
30
31
32
33
34
35
36
37
38
39 Neither total aboveground biomass nor percent cover of *P. schreberi* had any significant effect on
40 greenhouse gas fluxes in our models. We expected that N₂O emissions would increase as feathermoss
41 abundance (and associated N₂-fixation) has been shown to increase with TSF in these stands
42 (Zackrisson and others 2004) and because feathermosses such as *H. splendens* have been shown to
43 release N₂O (Lenhart and others 2015). It is possible that a decrease in nitrification and
44 ammonification in the soil (DeLuca and others 2002a) counteracted this somewhat, but also the *P.*
45 *schreberi* cover in our plots only ranged from 70-100%, which may not have been enough variation to
46 see an effect. Future work might include measurements of these processes along with N₂O emissions
47 to explore this further.

1
2
3 In this heterogeneous, high latitude landscape, micro-topography can greatly influence site conditions
4 and microclimate; for example, the low solar angle means that slope and aspect influence how much
5 solar radiation a stand can receive (Bonan and Shugart 1989). Similarly, Zackrisson (1977) noted that
6 stands on south-facing slopes in the Swedish boreal region experience more frequent fires than those
7 facing north. Several other factors contributing to soil and plant community compositions following
8 wildfire are important considerations. The intensity and severity of the burn greatly impact secondary
9 succession by influencing forest structure and the remaining nutrient pool (Flannigan and others 2005;
10 Lecomte and others 2006). For example, we know NJA (47 years since fire) experienced a high
11 severity, stand-replacing fire and now has much higher grass cover (data not shown) and fewer trees
12 (personal observation) than JAR, which burned only six years earlier. Moreover, stand structure prior
13 to burning partially dictates how severe the next fire might be (i.e. recently burned stands with less
14 organic material accumulated will likely experience a less severe burn than an old site with abundant
15 fuel). As well, the amount of charcoal remaining is important for enhancing soil fertility and
16 adsorption of allelopathic polyphenols following fire (Zackrisson and others 1996; DeLuca and others
17 2002a). Future work on *in situ* boreal forest floor GHG fluxes would benefit from measures of these
18 factors.
19
20
21
22
23
24
25
26
27
28
29
30
31
32
33
34
35
36
37
38
39
40

41 **Conclusion**

42
43
44
45 We predicted that there would be trends in soil properties, *P. schreberi* cover, and microbial
46 communities with increasing time since last wildfire disturbance and that these properties would
47 influence GHG emissions along our chronosequence. Our results show that boreal forest floor GHG
48 emissions are both site- and climate-driven, where site encompasses combinations of measured and
49 unmeasured factors (such as the intensity and severity of the last burn, the structure of the forest prior
50 to burning and adjacent to burn sites, and the amount of charcoal remaining). Climate, as indicated by
51 sampling period, was a strong driver of GHG fluxes but some soil properties (C:N, depth, and
52 moisture) were influential. Many studies show trends in ecosystem properties along boreal forest
53
54
55
56
57
58
59
60

1
2
3 wildfire chronosequences, but our study suggests that local heterogeneity in the landscape is a
4
5 powerful regulator of later successional forest floor GHG emissions and needs to be considered when
6
7 predicting the effects of more frequent, severe and extensive wildfires.
8
9

10 11 12 13 **Acknowledgements**

14
15
16
17
18 Funding for this research was provided by the Natural Environment Research Council, UK. We
19
20 would like to thank T. N. Walker, P. A. Henrys, and S. G. Jarvis for their guidance in statistical
21
22 analyses and use of R software, and Matt Clifford for his assistance in the laboratory analyses.
23
24 Special thanks to the kind staff at the Silvermuseet in Arjeplog for letting us share their space.
25
26
27
28
29

30 31 **References:**

- 32
33
34 Allison SD, Czimczik CI, Treseder KK. 2008. Microbial activity and soil respiration under nitrogen
35
36 addition in Alaskan boreal forest. *Global Change Biology* 14:1156–68.
37
38
39 Bartoń K. 2016. MuMIn: Multi-Model Interface. R package version 1.15.6.
40
41
42
43 Bligh EG, Dyer WJ. 1959. A rapid method of total lipid extraction and purification. *Canadian Journal*
44
45 *of Biochemistry and Physiology* 37:911–7.
46
47
48 Bonan GB, Shugart HH. 1989. Environmental Factors and Ecological Processes in Boreal Forests.
49
50 *Annual Review of Ecology and Systematics* 20:1–28.
51
52
53
54 Brais S, Camiré C, Bergeron Y, Paré D. 1995. Changes in nutrient availability and forest floor
55
56 characteristics in relation to stand age and forest composition in the southern part of the boreal
57
58 forest of northwestern Quebec. *Forest Ecology and Management* 76:181–9.
59
60

- 1
2
3 Briones MJJ, McNamara NP, Poskitt J, Crow SE, Ostle NJ. 2014. Interactive biotic and abiotic
4 regulators of soil carbon cycling: Evidence from controlled climate experiments on peatland and
5 boreal soils. *Global Change Biology* 20:2971–82.
6
7
8
9
10 Carcaillet C, Bergman I, Delorme S, Hornberg G, Zackrisson O. 2007. Long-term fire frequency not
11 linked to prehistoric occupation in northern Swedish boreal forest. *Ecology* 88:465–77.
12
13
14
15
16 Chapin FS III, Matson PA, Mooney HA. 2002. *Principles of Terrestrial Ecosystem Ecology*. New
17 York: Springer. 436 p.
18
19
20
21 Clemmensen KE, Bahr A, Ovaskainen O, Dahlberg A, Ekblad A, Wallander H, Stenlid J, Finlay RD,
22 Wardle DA, Lindahl BD. 2013. Roots and Associated Fungi Drive Long-Term Carbon
23 Sequestration in Boreal Forest. *Science* 339:1615–8.
24
25
26
27
28
29 Clemmensen KE, Finlay RD, Dahlberg A, Stenlid J, Wardle DA, Lindahl BD. 2015. Carbon
30 sequestration is related to mycorrhizal fungal community shifts during long-term succession in
31 boreal forests. *New Phytologist* 205:1525–36.
32
33
34
35
36
37 Crossman ZM, Abraham F, Evershed RP. 2004. Stable Isotope Pulse-Chasing and Compound
38 Specific Stable Carbon Isotope Analysis of Phospholipid Fatty Acids to Assess Methane
39 Oxidizing Bacterial Populations in Landfill Cover Soils. *Environmental Science and Technology*
40 38:1359–67.
41
42
43
44
45
46 de Groot WJ, Flannigan MD, Cantin AS. 2013. Climate change impacts on future boreal fire regimes.
47 *Forest Ecology and Management* 294:35–44.
48
49
50
51 de Vries FT, Manning P, Tallwin JRB, Mortimer SR, Pilgrim ES, Harrison KA, Hobbs PJ, Quirk H,
52 Shipley B, Cornelissen JHC, Kattge J, Bardgett RD. 2012. Abiotic drivers and plant traits
53 explain landscape-scale patterns in soil microbial communities. *Ecology Letters* 15:1230–9.
54
55
56
57
58
59
60

- 1
2
3 DeLuca TH, Nilsson M-C, Zackrisson O. 2002a. Nitrogen mineralization and phenol accumulation
4 along a fire chronosequence in northern Sweden. *Oecologia* 133:206–14.
5
6
7
8 DeLuca TH, Zackrisson O, Nilsson M-C, Sellstedt A. 2002b. Quantifying nitrogen-fixation in feather
9 moss carpets of boreal forests. *Letters to Nature* 419:917–20.
10
11
12
13 DeLuca TH, Sala A. 2006. Frequent Fire Alters Nitrogen Transformations in Ponderosa Pine Stands
14 of the Inland Northwest. *Ecology* 87:2511–22.
15
16
17
18 DeLuca TH, Zackrisson O, Gundale MJ, Nilsson M-C. 2008. Ecosystem feedbacks and nitrogen
19 fixation in boreal forests. *Science* 320:1181.
20
21
22
23 DeLuca TH, Boisvenue C. 2012. Boreal forest soil carbon: Distribution, function and modelling.
24
25
26
27
28
29
30 Engelman O. 1999. Boreal forest disturbance. In: R. L. Walker, editor. *Ecosystems of disturbed*
31
32
33
34
35
36
37
38
39
40
41
42
43 Flannigan M, Cantin AS, De Groot WJ, Wotton M, Newbery A, Gowman LM. 2013. Global wildland
44
45
46
47
48
49
50
51
52
53
54
55
56
57
58
59
60
- Flannigan MD, Amiro BD, Logan KA, Stocks BJ, Wotton BM. 2005. Forest Fires and Climate
Change in the 21ST Century. *Mitigation and Adaptation Strategies for Global Change* 11:847–
59.
- Girardin MP, Ali A, Carcaillet C, Mudelsee M, Drobyshev I, Hély C, Bergeron Y. 2009.
Heterogeneous response of circumboreal wildfire risk to climate change since the early 1900s.
Global Change Biology 15:2751–69.
- Harden JW, Mack M, Veldhuis H, Gower ST. 2002. Fire dynamics and implications for nitrogen
cycling in boreal forests. *Journal of Geophysical Research* 108:8223.

- 1
2
3 Hobbie SE, Nadelhoffer KJ, Högberg P. 2002. A synthesis: The role of nutrients as constraints on
4 carbon balances in boreal and arctic regions. *Plant and Soil* 242:163–70.
5
6
7
8
9 Holden SR, Gutierrez A, Treseder KK. 2013. Changes in Soil Fungal Communities, Extracellular
10 Enzyme Activities, and Litter Decomposition Across a Fire Chronosequence in Alaskan Boreal
11 Forests. *Ecosystems* 16:34–46.
12
13
14
15
16 Jonasson S, Michelsen A, Schmidt IK, Nielsen EV. 1999. Responses in microbes and plants to
17 changed temperature, nutrient, and light regimes in the arctic. *Ecology* 80:1828–43.
18
19
20
21 Kovats, RS, Valentini R, Bouwer LM, Georgopoulou E, Jacob D, Martin E, Rounsevell M, Soussana
22 J-F. 2014. Europe. In: Barros VR, Field CB, Dokken DJ, Mastrandrea MD, Mach KJ, Bilir TE,
23 Chatterjee M, Ebi KL, Estrada YO, Genova RC, Girma B, Kissel ES, Levy AN, MacCracken S,
24 Mastrandrea PR, White LL, editors. *Climate Change 2014: Impacts, Adaptation, and*
25 *Vulnerability. Part B: Regional Aspects. Contribution of Working Group II to the Fifth*
26 *Assessment Report of the Intergovernmental Panel on Climate Change.* Cambridge, UK and
27 New York, USA: Cambridge University Press. p1267–1326.
28
29
30
31
32
33
34
35
36
37 Lagerström A, Esberg C, Wardle DA, Giesler R. 2009. Soil phosphorus and microbial response to a
38 long-term wildfire chronosequence in northern Sweden. *Biogeochemistry* 95:199–213.
39
40
41
42
43 Lecomte N, Simard M, Fenton N, Bergeron Y. 2006. Fire Severity and Long-term Ecosystem
44 Biomass Dynamics in Coniferous Boreal Forests of Eastern Canada. *Ecosystems* 9:1215–30.
45
46
47
48 Lenhart K, Weber B, Elbert W, Steinkamp J, Clough T, Crutzen P, Pöschl U, Keppler F. 2015.
49 Nitrous oxide and methane emissions from cryptogamic covers. *Global Change Biology* 21:
50 3889–3900.
51
52
53
54
55
56 McNamara NP, Gregg R, Oakley S, Stott A, Rahman MT, Murrell JC, Wardle DA, Bardgett RD,
57 Ostle NJ. 2015. Soil Methane Sink Capacity Response to a Long-Term Wildfire
58 Chronosequence in Northern Sweden. *PLoS ONE* 10:e0129892.
59
60

- 1
2
3 Niklasson M, Granstrom A. 2013. Numbers and Sizes of Fires : Long-Term Spatially Explicit Fire
4
5 History in a Swedish Boreal Landscape. *Ecology* 81:1484–99.
6
7
- 8 Oechel WC, Van Cleve K. 1986. The Role of Bryophytes in Nutrient Cycling in the Taiga. In: Van
9
10 Cleve K, Chapin FS, Flanagan PW, Viereck LA, Dyrness CT, editors. *Forest Ecosystems in the*
11
12 *Alaskan Taiga: A Synthesis of Structure and Function*. New York: Springer-Verlag New York.
13
14 p121–37.
15
16
- 17
18 O'Neill KP, Kasischke ES, Richter DD. 2003. Seasonal and decadal patterns of soil carbon uptake
19
20 and emission along an age sequence of burned black spruce stands in interior Alaska. *Journal of*
21
22 *Geophysical Research* 108:8155.
23
24
- 25
26 Pan Y, Birdsey RA, Fang J, Houghton R, Kauppi PE, Kurz WA, Phillips OL, Shvidenko A, Lewis
27
28 SL, Canadell JG, Ciais P, Jackson RB, Pacala SW, McGuire AD, Piao S, Rautiainen A, Sitch S,
29
30 Hayes D. 2011. A large and persistent carbon sink in the world's forests. *Science* 333:988–93.
31
32
- 33
34 Paré D, Bergeron Y, Camiré C. 1993. Changes in the Forest Floor of Canadian Southern Boreal
35
36 Forest after Disturbance. *Journal of Vegetation Science* 4:811–8.
37
38
- 39
40 Pinheiro J, Bates D, DebRoy S, Sarkar D, R Core Team. 2015. nlme: Linear and Nonlinear
41
42 Mixed Effects Models. R package version 3.1-122.
43
44
- 45
46 Prescott CE, Maynard DG, Laiho R. 2000. Humus in northern forests: Friend or foe? *Forest Ecology*
47
48 *and Management* 133:23–36.
49
50
- 51
52 R Development Core Team. 2014. R: A language and environment for statistical computing. R
53
54 Foundation for Statistical Computing, Vienna, Austria. (Available at: <http://www.R-project.org/>).
55
56
- 57
58 Street LE, Subke J-A, Sommerkorn M, Sloan V, Ducrottoy H, Phoenix GK, Williams M. 2013. The
59
60 role of mosses in carbon uptake and partitioning in arctic vegetation. *New Phytologist* 199:163–
75.

- 1
2
3 Tjoelker MG, Oleksyn J, Reich PB, Żytkowiak R. 2008. Coupling of respiration, nitrogen, and sugars
4 underlies convergent temperature acclimation in *Pinus banksiana* across wide-ranging sites and
5 populations. *Global Change Biology* 14:782–97.
6
7
8
9
10
11 Van Cleve K, Sprague D. 2015. Respiration rates in the forest floor of birch and aspen stands in
12 interior Alaska. *Journal of Canadian Forest Research* 3:17–26.
13
14
15
16 Ward C, Pothier D, Paré D. 2014. Do boreal forests need fire disturbance to maintain productivity?
17 *Ecosystems* 17:1053–1067.
18
19
20
21 Ward SE, Ostle NJ, Oakley S, Quirk H, Henrys PA, Bardgett RD. 2013. Warming effects on
22 greenhouse gas fluxes in peatlands are modulated by vegetation composition. *Ecology Letters*
23 16:1285–93.
24
25
26
27
28
29 Wardle DA. 1997. The Influence of Island Area on Ecosystem Properties. *Science* 277:1296–9.
30
31
32 Wardle DA, Hörnberg G, Zackrisson O, Kalela-Brundin M, Coomes DA. 2003. Long-term effects of
33 wildfire on ecosystem properties across an island area gradient. *Science* 300:972–5.
34
35
36
37 Wardle DA, Zackrisson O. 2005. Effects of species and functional group loss on island ecosystem
38 properties. *Nature* 435:806–10.
39
40
41
42
43 Wardle DA, Jonsson M, Bansal S, Bardgett RD, Gundale MJ, Metcalfe DB. 2012a. Linking
44 vegetation change, carbon sequestration and biodiversity: Insights from island ecosystems in a
45 long-term natural experiment. *Journal of Ecology* 100:16–30.
46
47
48
49
50 Wardle DA, Jonsson M, Kalela-Brundin M, Lagerström A, Bardgett RD, Yeates GW, Nilsson MC.
51 2012b. Drivers of inter-year variability of plant production and decomposers across contrasting
52 island ecosystems. *Ecology* 93:521–31.
53
54
55
56
57
58
59
60

- 1
2
3 Whitaker J, Ostle N, Nottingham AT, Ccahuana A, Salinas N, Bardgett RD, Meir P, McNamara NP.
4
5 2014. Microbial community composition explains soil respiration responses to changing carbon
6
7 inputs along an Andes-to-Amazon elevation gradient. *Journal of Ecology* 102:1058–71.
8
9
10 Williams TG, Flanagan LB. 1996. Effect of changes in water content on photosynthesis, transpiration
11
12 and discrimination against $^{13}\text{CO}_2$ and $\text{C}^{18}\text{O}^{16}\text{O}$ in *Pleurozium* and *Sphagnum*. *Oecologia* 2:38–
13
14 46.
15
16
17
18 Zackrisson O. 1977. Influence of forest fires on the North Swedish boreal forest. *Oikos* 29:22–32.
19
20
21 Zackrisson O. 1980. Forest fire history: ecological significance and dating problems in the north
22
23 Swedish boreal forests. - In: Dietrich, JH, Stokes, M, editors. Proceedings of the fire history
24
25 workshop, University of Arizona. USDA, Rocky Mountain Forest and Experiment Station.
26
27 General Technical Report RM81, p120–125.
28
29
30
31 Zackrisson O, Nilsson M, Wardle DA. 1996. Ecological Function of Charcoal from Wildfire in the
32
33 Boreal Forest. *Oikos* 77:10–9.
34
35
36
37 Zackrisson O, DeLuca TH, Nilsson MC, Sellstedt A, Berglund LM. 2004. Nitrogen fixation increases
38
39 with successional age in boreal forests. *Ecology* 85:3327–34.
40
41
42 Zackrisson O, DeLuca TH, Gentili F, Sellstedt A, Jäderlund A. 2009. Nitrogen fixation in mixed
43
44 *Hylocomium splendens* moss communities. *Oecologia* 160:309–19.
45
46
47
48 Zuur AE, Ieno EN, Walker NJ, Saveliev AA, Smith GM. 2009. *Mixed Effects Models and Extensions*
49
50 *in Ecology with R*. New York: Springer. 574p.
51
52
53

Figure Captions

54
55
56 Figure 1. Significant (linear regression with time since fire) soil properties of the organic horizon
57
58 sampled within the gas chamber rings (blue circles) and along a separate transect (black dots) at
59
60 selected sites; dw = dry weight.

1
2
3 Figure 2. Mean greenhouse gas fluxes (\pm standard error) in each sampling campaign.
4

5
6 Figure S1. Non-significant (linear regression with time since fire) soil properties of the organic
7 horizon samples within the gas chamber rings (blue circles) and along a separate transect (black dots)
8 at selected sites; dw = dry weight, SOM = soil organic matter, PLFA = phospholipid fatty acid.
9

10 Figure S2. Linear regression results of final plant aboveground biomass and percent cover of
11 *Pleurozium schreberi* in the field plots at selected sites.
12
13
14
15
16
17
18
19
20
21
22
23
24
25
26
27
28
29
30
31
32
33
34
35
36
37
38
39
40
41
42
43
44
45
46
47
48
49
50
51
52
53
54
55
56
57
58
59
60

For Peer Review

Table 1. Summary information for sampling locations. Site ages are the time since fire as of 2014.

Site name	Site code	Location	Time since fire (years)
Njållatjivelg	NJA	65° 48' 54" N 19° 02' 07" E	47
Jarvliden	JAR	65° 34' 09" N 18° 24' 01" E	53
Laddok	LAD	65° 56' 43" N 18° 22' 37" E	136
Guorbåive	GUO	65° 48' 57" N 19° 02' 54" E	183
Fettjärn	FET	65° 55' 28" N 18° 29' 58" E	232
Reivo	REV	65° 46' 28" N 19° 06' 19" E	367

For Peer Review

1
2
3
4
5
6
7
8
9
10
11
12
13
14
15
16
17
18
19
20
21
22
23
24
25
26
27
28
29
30
31
32
33
34
35
36
37
38
39
40
41
42
43
44
45
46

Table 2. Summary of fixed factors initially included for LME model selection.

Factors Included in Model Selection	Mean	Standard Error	Range
Site (or Time Since Fire)* Soil Temperature (5 cm depth)	-	-	-
Site (or Time Since Fire)	169.67 years	23.18 years	47 – 367 years
Soil Temperature (5 cm depth)	9.26°C	0.60°C	5.26 – 15.78°C
Sampling Period	-	-	-
Photosynthetically Active Radiation (PAR)	79.41 $\mu\text{mol m}^{-2} \text{s}^{-1}$	38.47 $\mu\text{mol m}^{-2} \text{s}^{-1}$	2 – 1130 $\mu\text{mol m}^{-2} \text{s}^{-1}$
Soil Moisture	24%	1%	4 – 33%
Leaf Moisture	514.81 raw counts	25.27 raw counts	437 – 909.83 raw counts
Depth _{OH}	5.82 cm	0.57 cm	1.5 – 10.5 cm
C:N _{OH}	34.90	0.90	19.99 – 48.14
Total N _{OH}	7.15 mg g ⁻¹ soil	0.40 mg g ⁻¹ soil	2.74 – 12.54 mg g ⁻¹ soil
Final Aboveground Biomass	149.69 g	5.71 g	84.1 – 208.40 g
% Cover - <i>Pleurozium schreberi</i>	95.5%	1.39%	70 – 100%

After removal of collinear terms, these factors were included in the initial linear mixed effects models and subject to removal using a step-wise process. OH = Soil organic horizon.

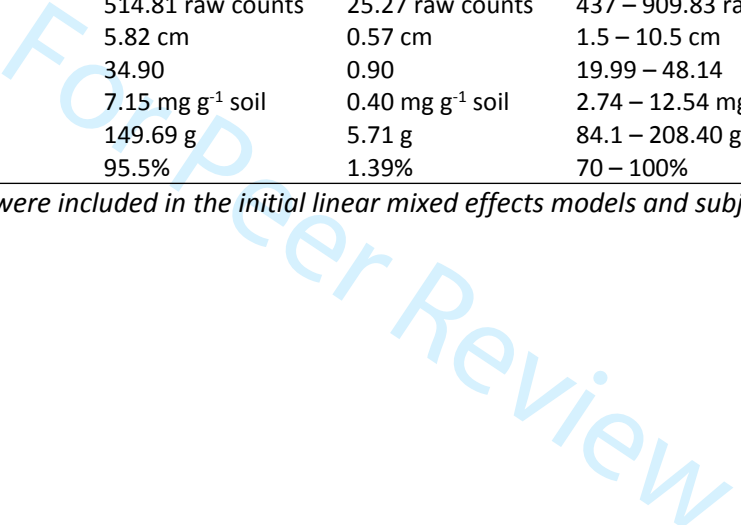


Table 3. Likelihood ratio deletion test results for selected models of greenhouse gas fluxes

	Ecosystem Respiration	Net Ecosystem Exchange	CH₄ Flux	N₂O Flux
	R ² _{marginal} = 0.642	R ² _{marginal} = 0.397	R ² _{marginal} = 0.299	R ² _{marginal} = 0.040
	R ² _{conditional} = 0.679	R ² _{conditional} = 0.489	R ² _{conditional} = 0.608	R ² _{conditional} = 0.040
	RMSE = 1.338	RMSE = 24.589	RMSE = 0.022	RMSE = 0.005
	Site*Soil Temperature _{5cm}	17.86, <i>df</i> = 15,20, <i>p</i> < 0.0013	-	-
	Site	21.24, <i>df</i> = 11,17, <i>p</i> < 0.0003	12.38, <i>df</i> = 9,15, <i>p</i> < 0.0148	10.06, <i>df</i> = 6,13, <i>p</i> < 0.0394
	Soil Temperature _{5cm}	5.13, <i>df</i> = 10,16, <i>p</i> = 0.0236	-	-
	Sampling Period	81.87, <i>df</i> = 11,17, <i>p</i> < 0.0001	43.54, <i>df</i> = 9,15, <i>p</i> < 0.0001	-
	PAR	-	-	-
Factor	Soil Moisture	22.78, <i>df</i> = 11,17, <i>p</i> < 0.0001	-	6.02, <i>df</i> = 6,13, <i>p</i> < 0.0141
	Leaf Moisture	24.80, <i>df</i> = 11,17, <i>p</i> < 0.0001	-	8.19, <i>df</i> = 6,13, <i>p</i> < 0.0042
	Depth _{OH}	-	8.55, <i>df</i> = 15,20, <i>p</i> < 0.0035	-
	C:N _{OH}	4.72, <i>df</i> = 11,17, <i>p</i> < 0.0299	-	-
	Total N _{OH}	-	-	-
	Final Plant Biomass	-	-	-
	% Cover – <i>P. schreberi</i>	-	-	-

Likelihood ratio deletion test results (LR, degrees of freedom (df), p-value) and model fit (marginal and conditional R², root mean square error (RMSE)) of linear mixed effects models of greenhouse gas (GHG) fluxes. The final model for each GHG was selected based on a step-wise routine using single term deletions combined with likelihood ratio testing. The LR and p-values for each variable are the results of likelihood ratio tests between the maximum likelihood estimations of the final model and the same final model with that variable removed. R² values and RMSE are from final models with restricted maximum likelihood estimations. PAR = photosynthetically active radiation, OH = soil organic horizon.

Table 4. Parameter estimates for selected LME models of greenhouse gas fluxes

	Ecosystem Respiration		Net Ecosystem Exchange		CH ₄ Flux		N ₂ O Flux	
	Parameter estimate (± SE)	p-value	Parameter estimate (± SE)	p-value	Parameter estimate (± SE)	p-value	Parameter estimate (± SE)	p-value
Intercept	3.924 ± 2.067	0.0606	27.686 ± 28.821	0.3389	-0.010 ± 0.013	0.4331	0.00264 (± 0.00281)	0.3497
Site*Soil Temperature _{scm}	-	-	-	-	-	-	-	-
JAR*Soil Temperature _{scm}	-	-	7.425 ± 2.119	0.0007	-	-	-	-
LAD*Soil Temperature _{scm}	-	-	15.938 ± 4.911	0.0016	-	-	-	-
FET*Soil Temperature _{scm}	-	-	3.592 ± 2.317	0.1240	-	-	-	-
REV*Soil Temperature _{scm}	-	-	5.567 ± 2.281	0.0163	-	-	-	-
Site								
JAR	-0.917 ± 0.552	0.1133	-27.353 ± 21.266	0.2138	0.006 ± 0.013	0.6619	-0.00060 (± 0.00165)	0.7206
LAD	0.752 ± 0.627	0.2455	-111.812 ± 39.599	0.0109	0.007 ± 0.013	0.5946	-0.00226 (± 0.00170)	0.1999
FET	3.228 ± 0.955	0.0032	19.294 ± 24.358	0.4381	0.040 ± 0.012	0.0043	-0.00577 (± 0.00198)	0.0087
REV	-0.286 ± 0.490	0.5666	-26.392 ± 23.237	0.2702	0.018 ± 0.012	0.1532	-0.00146 (± 0.00158)	0.3648
Soil Temperature _{scm}	-	-	-0.658 ± 3.140	0.8344	-	-	-	-
Factor								
Sampling Period								
Sept 2012	-1.752 ± 0.419	0.0001	-12.619 ± 8.270	0.1300	-0.016 ± 0.005	0.0012	-	-
June 2013	0.059 ± 0.457	0.8975	-47.146 ± 7.752	<0.0001	-0.010 ± 0.006	0.0656	-	-
July 2014	3.813 ± 0.544	<0.0001	-32.776 ± 14.908	0.0301	-0.036 ± 0.005	<0.0001	-	-
PAR	-	-	-	-	-	-	-	-
Soil Moisture	28.662 ± 5.698	<0.0001	-	-	-	-	-0.02417 ± 0.00994	0.0166
Leaf Moisture	-0.006 ± 0.001	<0.0001	-	-	-4.0 x 10 ⁻⁵ ± 1.5 x 10 ⁻⁵	0.0072	9.91 x 10 ⁻⁵ ± 3.38 x 10 ⁻⁶	0.0041
Depth _{OH}	-	-	-5.213 ± 1.847	0.0109	-	-	-	-
C:N _{OH}	-0.067 ± 0.032	0.0545	-	-	-	-	-	-
Total N _{OH}	-	-	-	-	-	-	-	-
Final Plant Biomass	-	-	-	-	-	-	-	-
% Cover – <i>P. schreberi</i>	-	-	-	-	-	-	-	-

Parameter estimates and p-values (restricted maximum likelihood estimated models) are based on comparisons to the intercept, which includes site NJA and sampling period June 2012. PAR= photosynthetically active radiation, OH = soil organic horizon.

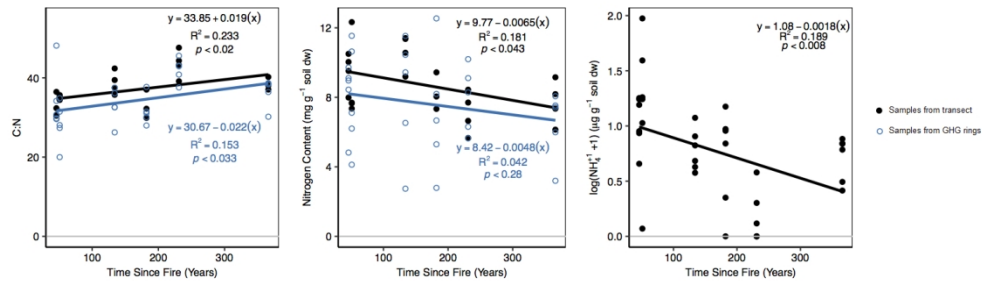


Figure 1. Significant (linear regression with time since fire) soil properties of the organic horizon sampled within the gas chamber rings (blue circles) and along a separate transect (black dots) at selected sites; dw = dry weight.

1
2
3
4
5
6
7
8
9
10
11
12
13
14
15
16
17
18
19
20
21
22
23
24
25
26
27
28
29
30
31
32
33
34
35
36
37
38
39
40
41
42
43
44
45
46
47
48
49
50
51
52
53
54
55
56
57
58
59
60

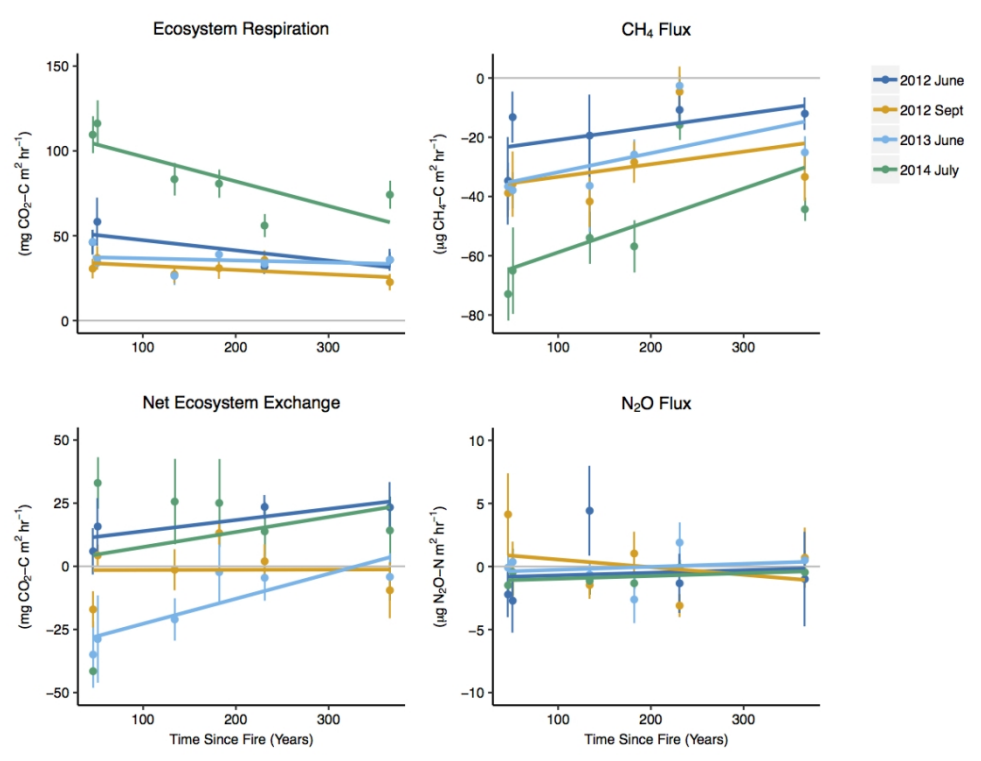


Figure 2. Mean greenhouse gas fluxes (± standard error) in each sampling campaign.

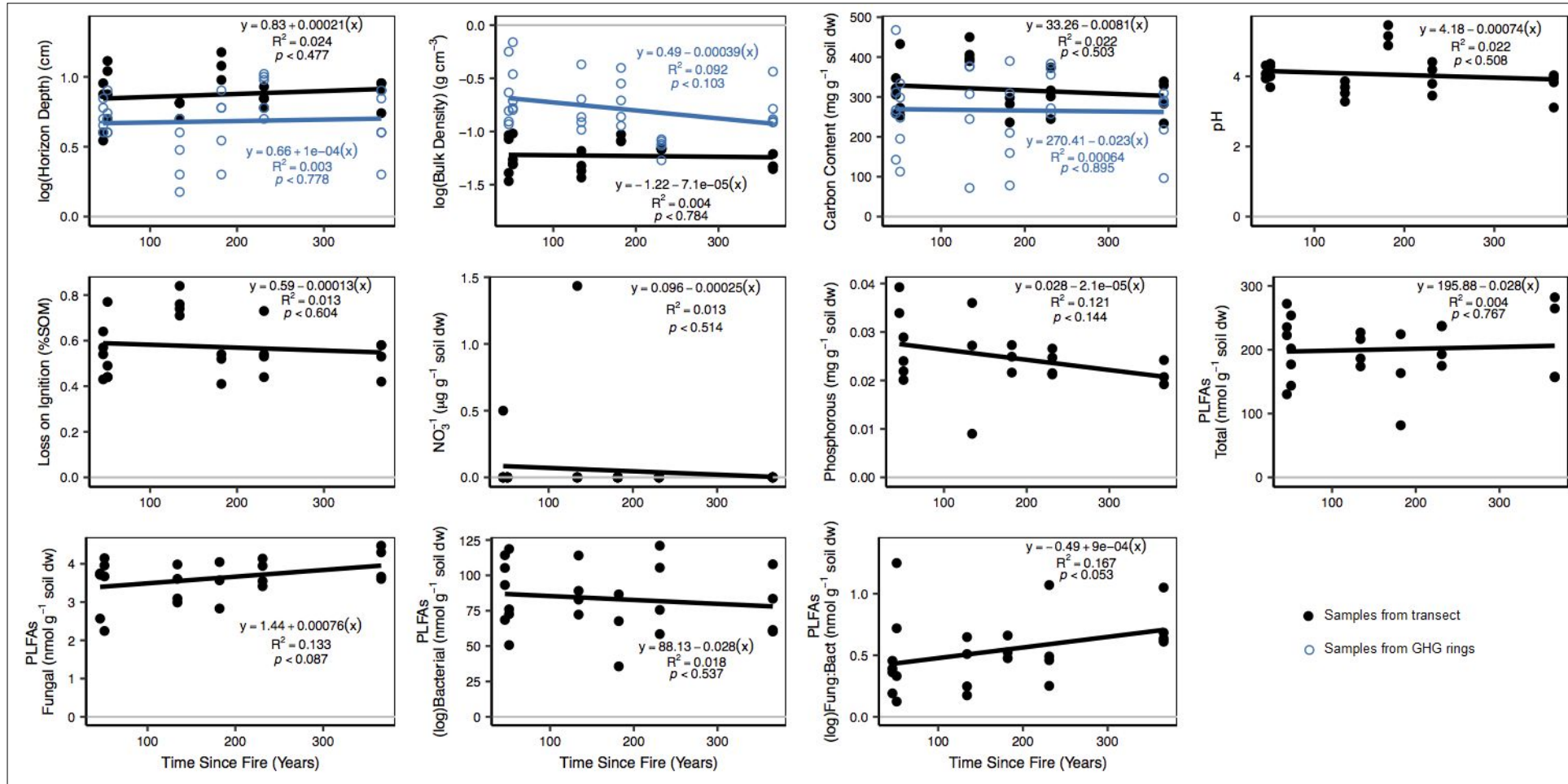


Figure S1. Non-significant (linear regression with time since fire) soil properties of the organic horizon samples within the gas chamber rings (blue circles) and along a separate transect (black dots) at selected sites; dw = dry weight, SOM = soil organic matter, PLFA = phospholipid fatty acid.

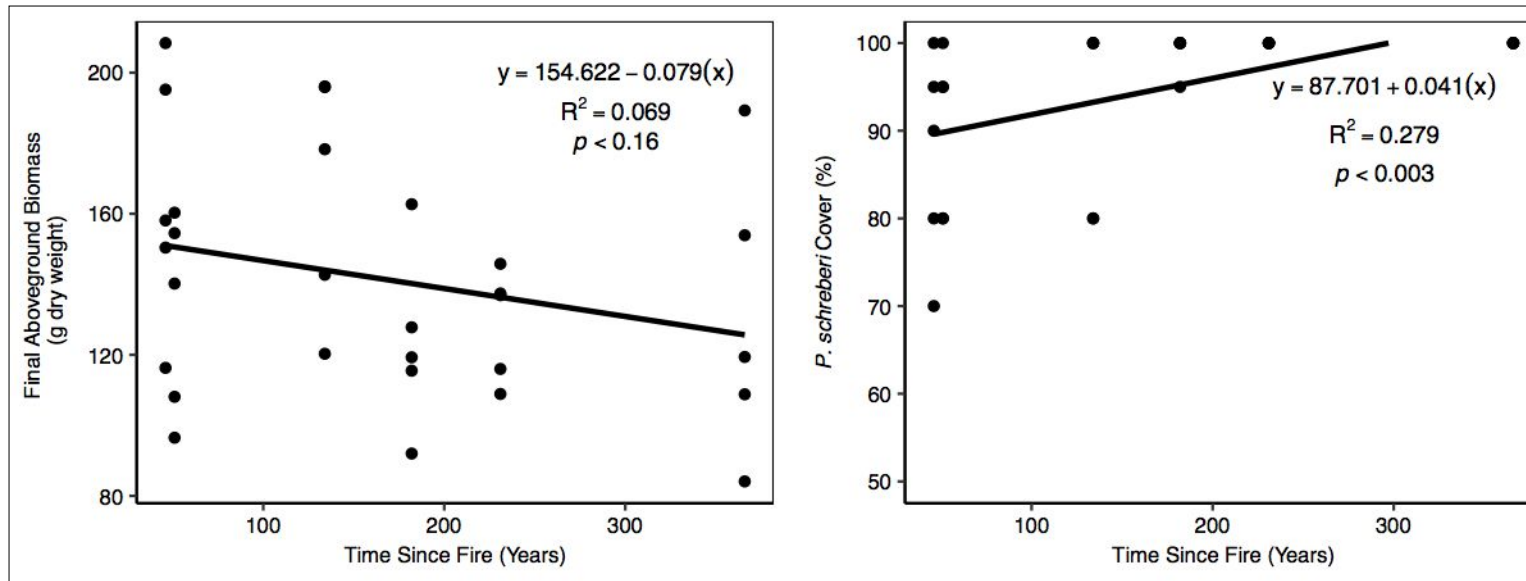


Figure S2. Linear regression results of final plant aboveground biomass and percent cover of *Pleurozium schreberi* in the field plots at selected sites.

Table S1. Likelihood ratio deletion test results for selected models of greenhouse gas fluxes (using time since fire in fixed effects selection)

	Ecosystem Respiration	Net Ecosystem Exchange	CH₄ Flux	N₂O Flux
	R ² _{marginal} = 0.593	R ² _{marginal} = 0.136	R ² _{marginal} = 0.307	No significant model
	R ² _{conditional} = 0.666	R ² _{conditional} = 0.335	R ² _{conditional} = 0.601	
	RMSE = 1.434	RMSE = 28.654	RMSE = 0.022	
Factor	Time Since Fire*Soil Temperature _{5cm}	-	-	-
	Time Since Fire	-	-	-
	Soil Temperature _{5cm}	7.55, <i>df</i> = 4,11, <i>p</i> = 0.0060	-	-
	Sampling Period	92.72, <i>df</i> = 5,12, <i>p</i> < 0.0001	26.49, <i>df</i> = 4,11, <i>p</i> < 0.0001	42.85, <i>df</i> = 9,16, <i>p</i> < 0.0001
	PAR	-	-	-
	Soil Moisture	93.08, <i>df</i> = 5,12, <i>p</i> < 0.0001	-	-
	Leaf Moisture	105.68, <i>df</i> = 5,12, <i>p</i> < 0.0001	-	7.26, <i>df</i> = 9,16, <i>p</i> = 0.0007
	Depth _{OH}	-	-	-
	C:N _{OH}	-	-	7.90, <i>df</i> = 9,16, <i>p</i> = 0.0049
	Total N _{OH}	-	-	4.87, <i>df</i> = 9,16, <i>p</i> = 0.0273
	Final Plant Biomass	-	-	-
	% Cover – <i>P. schreberi</i>	-	-	-

Likelihood ratio deletion test results (LR, degrees of freedom (df), p-value) and model fit (marginal and conditional R², root mean square error (RMSE)) of linear mixed effects models of greenhouse gas (GHG) fluxes where time since fire was included in fixed effects selection. The final model for each GHG was selected based on a step-wise routine using single term deletions combined with likelihood ratio testing. The LR and p-values for each variable are the results of likelihood ratio tests between the maximum likelihood estimations of the final model and the same final model with that variable removed. R² values and RMSE are from final models with restricted maximum likelihood estimations. PAR = photosynthetically active radiation, OH = soil organic horizon.

Table S2. Parameter estimates for selected LME models of greenhouse gas fluxes (using time since fire in fixed effects selection)

	Ecosystem Respiration – Log ₁₀		Net Ecosystem Exchange		CH ₄ Flux		N ₂ O Flux	
	Parameter estimate (± SE)	p-value	Parameter estimate (± SE)	p-value	Parameter estimate (± SE)	p-value	Parameter estimate (± SE)	p-value
Intercept	5.649 ± 1.024	<0.0001	-40.583 ± 20.503	0.0602	-0.046 ± 0.023	0.0539	-	-
Time Since Fire*Soil Temperature _{scm}	-	-	-	-	-	-	-	-
Time Since Fire	-	-	-	-	-	-	-	-
Soil Temperature _{scm}	-	-	6.658 ± 2.266	0.0040	-	-	-	-
Sampling Period								
Sept 2012	-1.577 ± 0.419	0.0003	-6.555 ± 8.525	0.4436	-0.015 ± 0.005	0.0013	-	-
June 2013	-0.391 ± 0.449	0.3852	-39.028 ± 7.722	<0.0001	-0.010 ± 0.006	0.0688	-	-
July 2014	2.924 ± 0.486	<0.0001	-42.874 ± 14.422	0.0036	-0.036 ± 0.005	<0.0001	-	-
Factor								
PAR	-	-	-	-	-	-	-	-
Soil Moisture	13.270 ± 2.862	<0.0001	-	-	-	-	-	-
Leaf Moisture	-0.005 ± 0.001	<0.0001	-	-	-4.08 × 10 ⁻⁵ ± 1.47 × 10 ⁻⁵	0.0066	-	-
Depth _{OH}	-	-	-	-	-	-	-	-
C:N _{OH}	-	-	-	-	0.0017 ± 0.0006	0.0086	-	-
Total N _{OH}	-	-	-	-	-0.0008 ± 0.0004	0.0405	-	-
Final Plant Biomass	-	-	-	-	-	-	-	-
% Cover – <i>P. schreberi</i>	-	-	-	-	-	-	-	-

Parameter estimates and p-values (restricted maximum likelihood estimated models) are based on comparisons to the intercept, which includes sampling period June 2012.

PAR= photosynthetically active radiation, OH = soil organic horizon.